Fifth International Symposium on Marine Propulsors
smp'17, Espoo, Finland, June 2017

Humpback whale inspired design for tidal turbine blades

Weichao Shi [1,2,*], Mehmet Atlar[2], Rosemary Norman[1]

[1]School of Marine Science and Technology, Newcastle University, UK
[2] Department of Naval Architecture, Ocean & Marine Engineering, University of Strathclyde, UK

ABSTRACT
This study is to further improve the hydrodynamic performance of tidal turbines by applying leading-edge tubercles to the blades inspired by the humpback whales.

The study first focused on the design and optimisation of the leading edge tubercles for a specific tidal turbine blade section by using numerical methods to propose an "optimum" design for the blade section. This optimum design was then applied onto a representative tidal turbine blade. This representative 3D blade demonstrated significant benefits especially after stall. The experimental measurements were further validated and complimented by numerical simulations using commercial CFD software for the detailed flow analysis.

Following that, a set of tidal turbine models with different leading-edge profiles was manufactured and series of model test campaigns were conducted in the cavitation tunnel to evaluate their efficiency, cavitation, underwater noise, and detailed flow characteristics. Based on these experimental investigations it was confirmed that the leading edge tubercles can improve: the hydrodynamic performance in the low Tip Speed Ratio (TSR) region without lowering the maximum power coefficient; constrain the cavitation development to within the troughs of the tubercles; and hence mitigating the underwater noise levels.

Keywords
Tidal turbine;·Blade design;·Leading-edge tubercles; Biomimetic

1 INTRODUCTION

Learning from the Mother Nature is a never stopped process for modern technology development. Recently the tubercles on the leading edges of humpback whale flippers have drawn the attention of researchers working in the field of tidal energy and wind energy, as these round protuberances along the leading edges have the ability to delay the stall and hence improve the lift-to-drag ratio of blades [1-6]. Many research studies, which are both numerical and experimental in nature, have investigated the influence of the leading-edge tubercles as applied on air fans, wind turbines, rudders and so on [6-10]. According to these studies, blades with leading-edge tubercles can maintain lift coefficients further beyond the stall point in comparison to those without tubercles.

1. Based on the above findings, the tubercles might be able to provide the tidal turbine blades with the following hydrodynamic advantages:
2. Better lift-to-drag ratio: This particular characteristic might be able to enhance the maximum power coefficient to help the turbine generate more power and more use of the available energy;
3. Delaying the stall angle: This factor might be able to help the turbine to operate more stably without the sudden loss of the lift which may cause fluctuation in power generation hence lowering the power quality. This may in turn cause the vibration and fatigue problems that reduce the lifetime of a tidal turbine.

Maintaining the lift under stall: This is another factor which might be very effective in the starting process of the fixed pitch tidal turbines as this process purely relies on the initial torque of the turbine to overcome the frictional torque and to start spinning. Since the initial torque is very small due to the high angle of attack, maintaining the lift under high angle of attack is crucial.

The above reviewed developments and technical observations have motivated this study to explore and develop this biomimetic concept further with a view to improve the hydrodynamic performance of the tidal turbines. Even though with such potential that tidal turbine might benefit from, it has been found that "extremely limited amount of research available for the application of the leading-edge tubercles on a tidal turbine". This will require further research, in particular experimental research, to help in understanding the physics of the leading-edge tubercles whether they can improve the turbine performance.

Within this framework, this project first focused on a tubercle design and optimization, which is described in

* Corresponding author: Weichao Shi, Weichao.shi@strath.ac.uk

Chapter 2. By conducting fundamental experimental and numerical investigations on the representative tidal turbine blade, the leading-edge tubercles demonstrated significant benefits, which is further elaborated in Chapter 3. Following the confidence built on the results of the representative turbine blade, a series of model testing campaign with the three tidal turbine models to explore the effect of leading-edge tubercles on the turbines has been conducted and results have been presented and discussed in Chapter 4. In Chapter 5, the findings in the representative turbine blade and the turbine models are liaised to summarize the major impact of applying leading-edge tubercles onto the tidal turbine.

2 TUBERCLE DESIGN AND OPTIMISATION

2.1 Description of Selected Tidal Turbine

The study was based on a previous UK National research programme (EPSRC-RNET), in which a tidal turbine was designed based on the S814 profile cross-section from the NREL series(Pham, Clelland, Grant, Varyani, & Barltrop, 2006; Wang, Atlar, & Sampson, 2007), as shown in Fig. 1. The key parameter is given in Table 1.

Table 1. Main particulars of the tidal stream turbine model (D=400mm)

r/R	*Chord length(mm)*	*Pitch angle (deg)*
0.2	64.35	27
0.3	60.06	15
0.4	55.76	7.5
0.5	51.47	4
0.6	47.18	2
0.7	42.88	0.5
0.8	38.59	-0.4
0.9	34.29	-1.3
1	30	-2

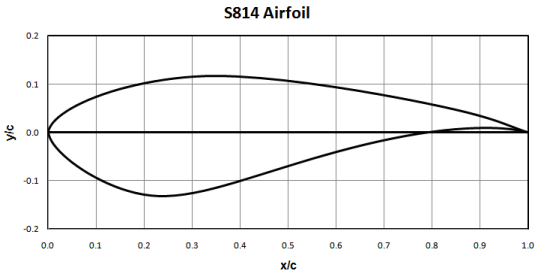

Fig. 1 Cross-section profile of S814

2.2 Tubercle profile design

Previous studies on the 2D foils were more focused on the optimisation of the sinusoidal shape tubercle profiles defined by different parameters, because of the close pattern with the specimen (K. Hansen, Kelso, & Doolan, 2012; K. L. Hansen, Kelso, & Dally, 2009; K. L. Hansen, Kelso, & Dally, 2011; K. L. Hansen, Rostamzadeh, Kelso, & Dally, 2016; Stanway, 2008; Swanson & Isaac, 2011; van Nierop, Alben, & Brenner, 2008). However, the current literature does not display any useful application of the leading-edge tubercles on thick and highly cambered tidal turbine foil section like the S814 section used in this study.

Therefore, combined with the experience from the previous studies, the sinusoidal form of tubercles was selected as the basis shape to conduct the numerical optimisation process. The investigation into the optimisation of the tubercle profiles was initiated by systematically changing two variants, the Height (H) and the Wavelength (W), of these protrusions based on the sinusoidal form of their shapes. The definitions of these parameters are shown in Fig. 2. The leading-edge profile is defined as in Equation 1.

$$h = \frac{H}{2}\cos\left[\frac{2\pi}{W}s - \pi\right] + \frac{H}{2} \quad (1)$$

where h (mm) is the local height of the leading-edge profile of tubercle relative to the reference one which is the smooth leading-edge profile; s (mm) is the spanwise position of foil section.

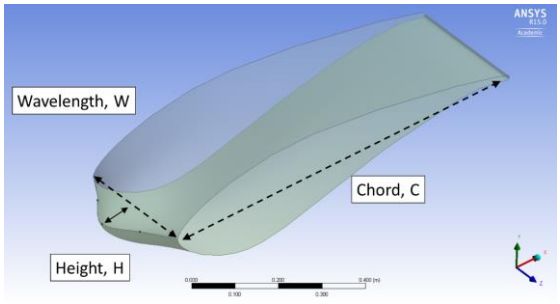

Fig. 2 Definition of 2D foil with a sinusoidal tubercle

2.3 Optimization Methodology

Numerical optimization of leading-edge tubercles for a 2D foil section S814 (with the representative profile section of S814) is the pathway to find the optimum design. With the changing variants, the models were built, meshed and evaluated all in the integrated environment of ANSYS-Workbench, which includes ANSYS-Designmodeller as a geometry generator, ANSYS-Meshing as a mesh generator and ANSYS-CFX as a CFD code for performance evaluation.

2.4 Optimum design of tubercles for S814

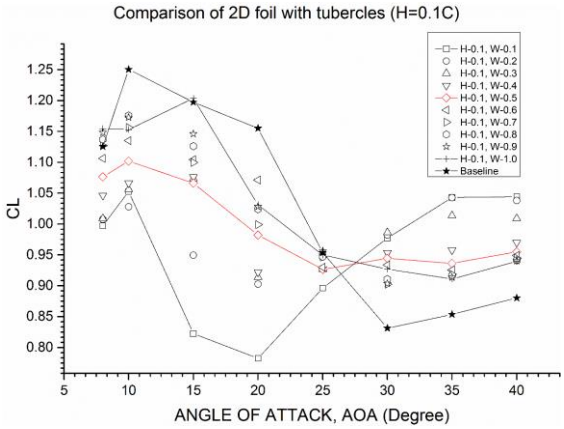

Fig. 3 Comparison of 2D foil lift coefficients with different tubercle profiles by varying the wavelength (W) at constant tubercle height (H=0.1C) (Shi, Atlar, et al., 2016)

The study was documented in detail as in reference (Shi, Atlar, Norman, Aktas, & Turkmen, 2016). Based on the optimisation study for the 2D foil section, a sinusoidal form of leading-edge tubercle profile with *0.1C* height and *0.5C* wavelength appeared to be a good compromise for an optimum design as the maintained lift over the varied

angles of attack (marked red in Fig. 3) at a price of slightly lowering the maximum C_L (defined in Equation 2).

$$C_L = \frac{Lift}{\frac{1}{2}\rho V^2 A} \quad (2)$$

where *Lift* is the lift of the foil which is perpendicular to the incoming flow; ρ is the density of the water; V is the inflow velocity; A is the reference area of the foil, which is C (Chord) * W (Wavelength).

3 APPLIED ON A REPRESENTATIVE TURBINE BLADE

Having conducted the numerical optimization of leading-edge tubercles for a 2D foil, the next task of this research was to apply the optimized tubercle shapes onto a 3D representative tidal turbine blade to understand the impact of the tidal turbine blade (Shi, Atlar, et al., 2016).

The representative 3D blade was based on the blade of the tidal turbine which had the same chord length distribution but a constant pitch. Via changing the angles of attack (AOAs), performance of the representative 3D blade is similar to the tidal turbine operating at varying tip speed ratios (TSRs). According the optimized tubercle design, the height of tubercle is set to be 10% of the local chord length while 8 tubercles can be evenly distributed along the span with the width settled to be 50% of the reference chord length which is corresponding to the 0.7R of the turbine blade.

3.1 Experimental investigation of the blade with the optimised tubercles

The 3D turbine blade was tested in the Emerson Cavitation Tunnel which is a medium size propeller testing water channel, for performance evaluation and flow measurement. Various combinations of the leading-edge profiles with changing the tubercle coverage shown in Fig. 4 were evaluated.

Based on the force measurement of lift and drag, the comparisons of the lift-to-drag ratios appears that Foil "0001", which had 1/4 of its leading-edge covered with tubercles, displayed an overall better performance. This can be clearly seen in Fig. 5 where Foil "0001" shows a positive impact from 0° to 26° AOA with more than 10% enhancement in the maximum lift-to-drag ratio at 5° AOA, compared to the reference (Foil "0000"). Even though Foil "1111" displayed the highest growth rate at 16° AOA, Foil "0001" may offer more potential in improving the performance of a tidal turbine operating over a wider range of tip speed ratios.

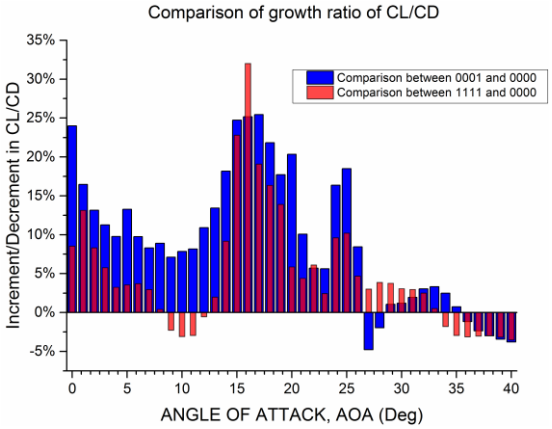

Fig. 5 Comparison of relative growth ratios for C_L/C_D for Foil "1111" (with leading-edge tubercles applied on whole span) and Foil "0001" (with minimum leading-edge tubercles applied around the tip)

During the flow visualization, the most striking difference between the flow around Foil "0000" and Foil "1111", was the development of a very strong tip vortex cavitation generated by Foil "0000" as opposed to almost no such cavitation generated by Foil "1111" due to the effect of the leading-edge tubercles. A close-up of this cavitating vortex, which emanated from the tip of the reference foil "0000" with about a 10mm diameter, is shown in Fig. 6.

Using a typical cavitating Rankine vortex expression, the relationship between the diameter of the cavitating tip vortex, a_c, and its circulation, Γ, can be given by Equation 3.

$$p_\infty - p_v = \frac{0.5\rho\Gamma^2}{4\pi^2 a_c^2} \quad (3)$$

where p_∞ is the pressure in far field and p_v is the saturated vapour pressure of the water.

According to Equation 3, the larger the diameter is, the stronger the vorticity. Since both foils were tested under the same conditions, the larger tip vortex cavitation experienced by the reference foil would be responsible for the stronger 3 dimensional effect and hence greater loss of

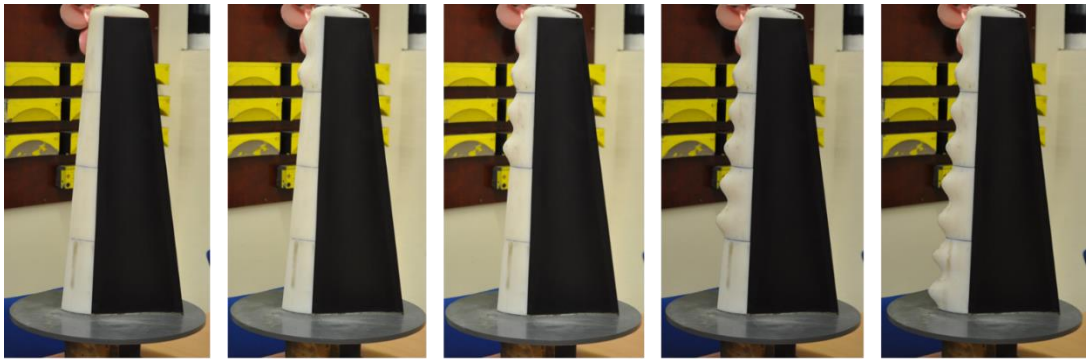

Fig. 4 Tested 3D hydrofoil models with interchangeable leading-edge parts

lift. whereas its counterpart (Foil "1111") with the leading-edge tubercles would maintain the 2D flow by lowering the end effect and therefore experience more favourable lift characteristics for the same condition.

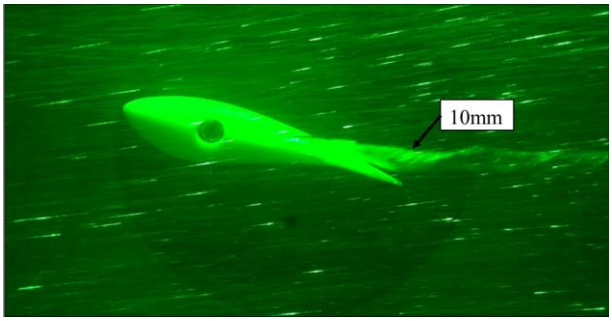

Fig. 6 Cavitating tip vortex observation on reference foil with smooth leading edge (Note a 10mm diameter tip vortex cavitation was generated)

3.2 Numerical simulation of the blade with the optimised tubercles

Following the experimental investigation, CFD simulations were conducted to complement to provide further details of the flow field and hence to understand the effect of tubercles. The simulations were conducted by Star-CCM+ to solve the incompressible Navier–Stokes equations with Detached Eddy Simulation (DES) models in order to take into account both vortex resolution and computational economy.

The CFD simulation domain was described and dimensioned according to the experimental environment, i.e. the measuring section of the ECT, as shown in Fig. 7. Taking advantage of the automatic polyhedral mesher, 21 million mesh has been generated.

The simulation has shown a good agreement with the experimental data. The comparison of the CFD predicted flow separation patterns at AOA=16º for Foil "0000" and Foil "1111" are shown in Fig. 8 by the iso-surface representations for the axial velocity (Vx) is equal to 0m/s. It can be clearly seen that the iso-surface of the reference hydrofoil was all connected together and formed into a huge cloud while the one of the tubercles hydrofoil was separated and containerised by the effect of the leading-edge tubercles. In addition, the separated volume was much smaller than that observed for Foil "0000".

Further demonstration the vortex activity on the foil surfaces in Fig. 9 shows that the vorticity [i] distribution on the suction side, indicates a pair of contra-rotating vortices generated from the tubercles along the span of the hydrofoil. By scrutinizing the details of the vorticity [i] distribution at the tip of the hydrofoil, the secret of why the leading-edge tubercles always perform better revealed. The contra-rotating vortices generated by these tubercles were interacting with the tip vortex by stopping it from spreading on the surface of the hydrofoil. As shown in Fig. 10, a vortex generated by tubercle next to the tip, which shows a positive vorticity [i] along a span position of Z=0.525 to 0.56 cancelled the strong negative tip vortex. As a result the detrimental effect of the tip vortex that would be responsible for the performance loss was greatly weakened.

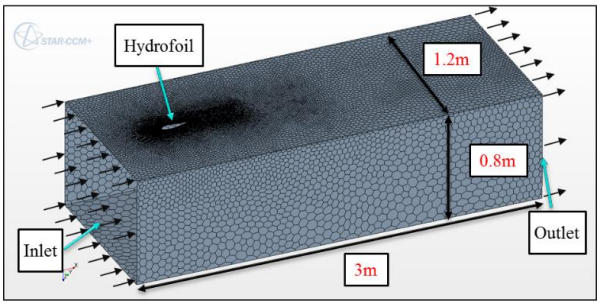

Fig. 7 Computation domain and boundary conditions

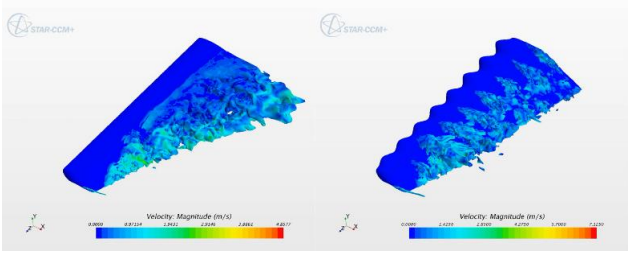

Fig. 8 Comparative flow separation patterns of two hydrofoils (Iso-surface: Vx=0m/s; AOA=16º)

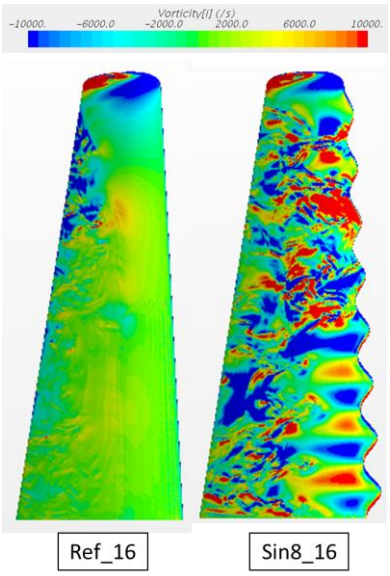

Fig. 9 Comparative vorticity [i] distributions along two hydrofoils on the suction side

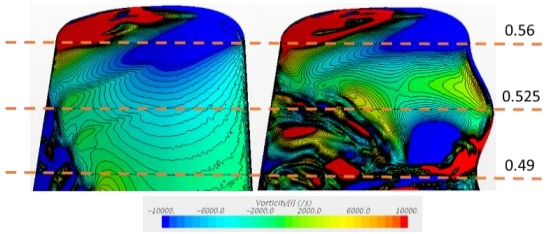

Fig. 10 Comparative details of vorticity [i] distribution at the suction side and tip of two hydrofoils

4 EXPERIMENTAL INVESTIGATIONS OF LEADING-EDGE TUBERCLES AS APPLIED ON TIDAL TURBINE

Following the confidence built on the results of the leading-edge tubercles as applied to the foil section and the representative turbine blade, the next step was to

investigate whether this biomimetic concept can be effective for improving the hydrodynamic performance of a state-of-the-art tidal turbine with the actual models. The test campaign includes: 1. open water performance tests; 2. cavitation observation tests; 3. noise measurement tests and 4. detailed flow measurement tests, which were all conducted in the ECT by the state-of-the-art model testing equipment. During the test various non-dimensional parameters have been used, listed as follow:

Power Coefficient: $$Cp = \frac{Q\omega}{\frac{1}{2}\rho A_T V^3} \quad (4)$$

Thrust Coefficient: $$C_T/10 = \frac{T}{\frac{1}{2}\rho A_T V^2}/10 \quad (5)$$

Tip Speed Ratio: $$TSR = \frac{\omega r}{V} \quad (6)$$

Reynolds Number: $$Re_{0.7r} = \frac{C_{0.7r}\sqrt{(V^2+(0.7\omega r)^2}}{\nu} \quad (7)$$

Cavitation Number: $$Cav_{0.7r} = \frac{P_{0.7r}-P_v}{\frac{1}{2}\rho\sqrt{(V^2+(0.7\omega r)^2}} \quad (8)$$

where Q is the torque of the turbine, Nm; T is the thrust, N; ω is the rotational speed, rad/s; A_T is the swept area of the turbine and equal $\pi D^2/4$, m^2; ρ is the tunnel water density, kg/m^3; V is the incoming velocity, m/s, D is the turbine diameter, m; $C_{0.7r}$is the chord length of the turbine at 0.7 radius, m; ν is the kinematic viscosity of the water, m^2/s; $P_{0.7r}$ is the static pressure at the upper 0.7 radius of the turbine, Pa; P_v is the vapour pressure of the water, Pa.

Based on the tubercle design and results of the blade tests, the three pitch adjustable turbine models with different leading-edge profiles were manufactured by Centrum Techniki Okrętowej S.A. (CTO, Gdansk), as shown **Error! Reference source not found.**. The reference turbine model with smooth leading edge (i.e. without tubercles) was named "Ref" to be used as the baseline. The one with two leading-edge tubercles at the tip, as shown in the middle of **Error! Reference source not found.**, was named as "Sin_2", which performed as the most efficient design in the representative blade tests. And the one with eight leading-edge tubercles was named as "Sin_8" which presented the maximum lift coefficient in the representative blade tests.

4.1 Open water hydrodynamic performance tests

The typical performance difference can be observed in Fig. 12. The top two plots show the power coefficients (Cp) and the thrust coefficients (Ct/10) and the bottom two plots show the comparison of different leading-edge tubercle profiles against the reference turbine. It can be seen that the leading-edge tubercles can improve the performance of the turbine in the lower range of TSRs (0.5 to 2.5), where the turbine is suffering from stall. Under these conditions, a turbine with leading-edge tubercles can generate more force, which can be observed in both Cp and Ct/10. Around 40% more torque can be achieved due to the lead-edge tubercles. However, with the increase in TSR, the Cp values of the Ref turbine and Sin_2 turbine reach a maximum value of 0.43, at TSR=3.5, while the turbine Sin_8 reached its maximum with a small delay at TSR=4. At the higher end of TSRs, turbines Sin_2 and Sin_8 can generate around 15 to 20% more torque and around 4% less thrust with the influence caused by Sin_8 more obvious than that of Sin_2. The experimental setup and the detailed result has all been documented in reference (Shi, Rosli, et al., 2016), while the results of other condition is very similar to result shown in Fig. 12.

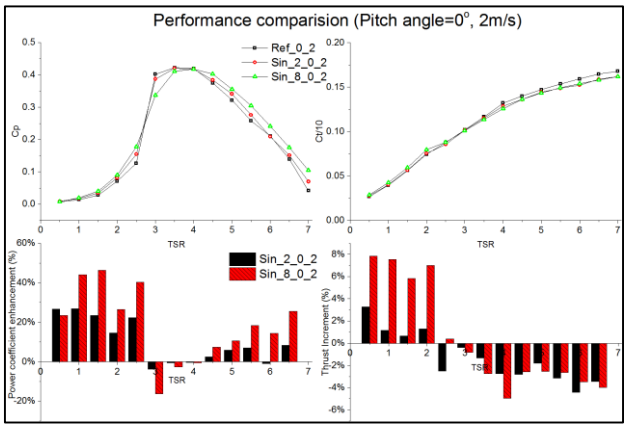

Fig. 12 Performance comparison (Pitch=0°, 2m/s)

4.2 Cavitation observation tests

In terms of the blade cavitation, two main types of cavitation pattern were noted once the cavitation was incepted. These were tip vortex cavitation and cloud cavitation with a misty appearance at the back or face side of the blade depending on the TSR.

The cavitation inception diagram is presented in Fig. 13. The sequence of these cavitation development on the blades was such that first the tip vortex cavitation appeared due to the higher resultant velocity at the tip in a steady manner. Then the tip vortex cavitation was gradually accompanied by a rather misty appearance of unsteady cloud cavitation on either side of the turbine blade depending on the TSR. While the cloud cavitation would

Fig. 11 Tested turbine models

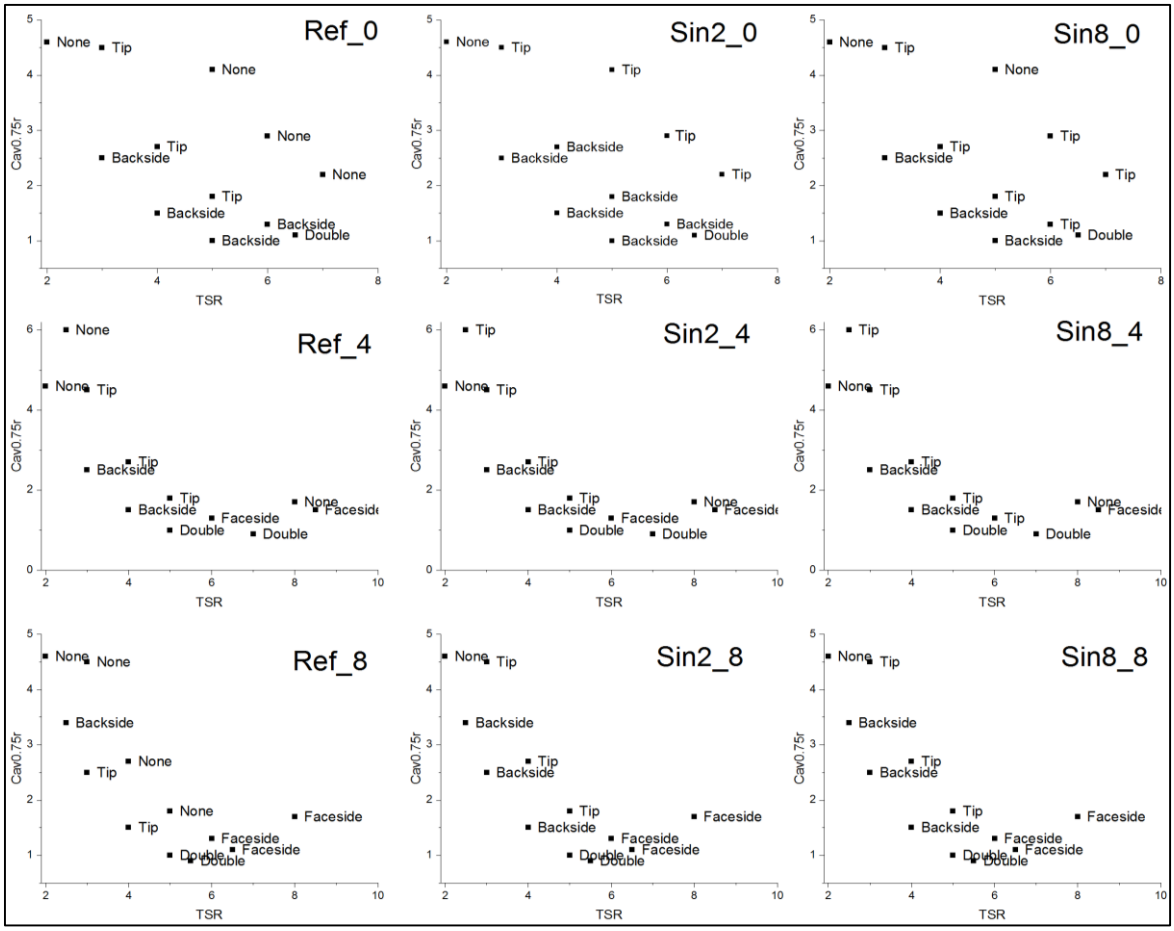

Fig. 13 Cavitation inception diagram

affect the turbine efficiency, the tip vortex cavitation did not have much impact on it.

On the other hand, the leading-edge tubercles may trigger earlier inception for the tip vortex cavitation compared to that for the reference turbine with the smooth leading edge. The strength of the tip vortex cavitation appeared to be similar for the different leading-edge profiles.

However, the development of the misty type cloud cavitation over the leading-edge tubercles was restricted to the trough areas of the tubercles, as shown in Fig. 14. This resulted in reduced cavitation extent and rather intermittent cavitation as opposed to the larger extent and continuous appearance of the cloud cavitation observed with the reference turbine.

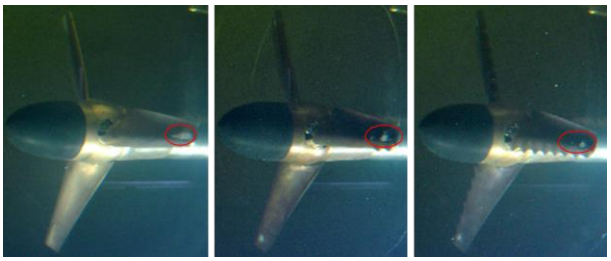

Fig. 14 Detailed comparison of cavitation pattern (Pitch angle=+8°; V=3m/s; TSR=6; $Cav_{0.75r}$=1.3)

4.3 Noise measurement tests

Together with the cavitation observation test, the underwater radiated noise level is also measured. The noise measurement result in Fig. 15 was analysed with the cavitation inception diagram in Fig. 13 to correlate the cavitation development with the noise level.

The three turbines displayed almost similar total noise levels until the cavitation was incepted. It can be seen from the top three plots in Fig. 15 (TSR<=2). Once the cavitation was incepted as noticed in Fig. 13, the noise levels of the turbines with tubercles (3<=TSR<=5) are generally higher than those of the reference turbine because of the early inception of the tip cavitation.

For the last condition in which all the three turbines were suffering from cloud cavitation, as shown in Fig. 15 (for TSR=6), the noise level of the Reference turbine in the higher frequency range from 3 KHz onwards was higher than that of the turbines with the leading-edge tubercles. This was because the face side cloud cavitation that was produced by the reference turbine had a larger extent and volume than that of the cavitation produced by the turbines Sin2 and Sin8. In Fig. 14 it can be easily seen that the face side cloud cavitation generated by the reference turbine has the largest extent while with the increase of the number of tubercles, the extent of cavitation is gradually reduced.

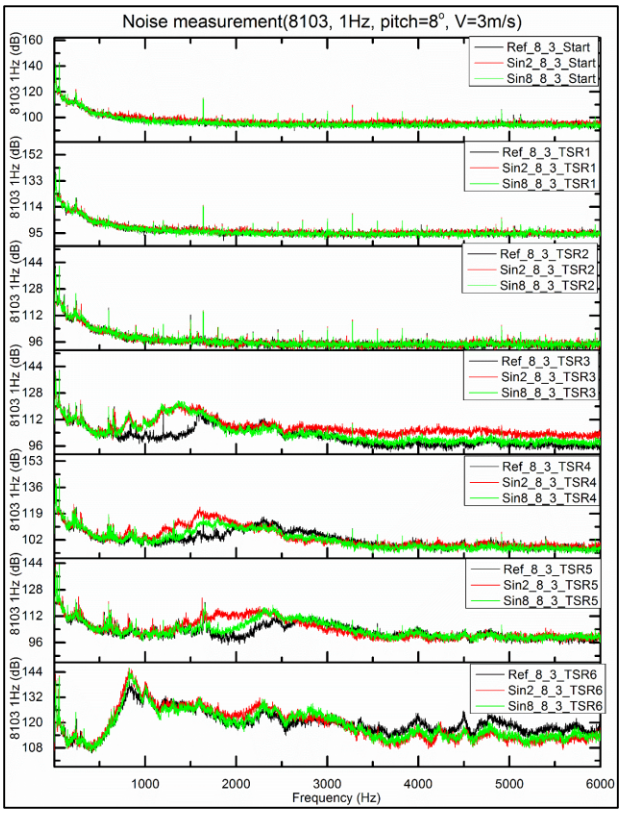

Fig. 15 Comparative total noise levels measured in 1Hz band (Pitch angle=8^0, V=3m/s)

4.4 Detailed flow measurement tests

Having investigated the effect of the leading-edge tubercles on the various performance characteristics of the tidal turbine blades, significant differences were observed requiring further explanation. The most fundamental and perhaps effective explanations could be made by conducting a detailed flow investigation around the turbine blades and slipstream of the turbines, preferably, by using a state-of-the-art Stereo Particle Image Velocimetry (SPIV) system.

Based on the measurement results of the blade cross-section under the "Stall condition", while all the tested turbine blades suffered from severe flow separations, the turbine blades with the leading-edge tubercles were able to maintain the flow to be more attached to their surfaces at certain positions, as seen in Fig. 16. This provided the turbine with additional torque for starting, as shown in the observed Cp benefits in lower TSRs.

On the other hand, the flow structure measured downstream of the turbine revealed that the turbines with tubercles can induce a higher induction factor, which resulted in lower velocities in the wake field as shown in the comparison of Figure 17 to Figure 19. This effect is positively related to the number of tubercles, which result in higher power coefficients (2.2% for Sin2 and 4.3% for Sin8) and also higher thrust coefficients (4.6% for Sin2 and 7.7% for Sin8) at this specific condition with the optimum TSR (TSR=4 and V=3m/s).

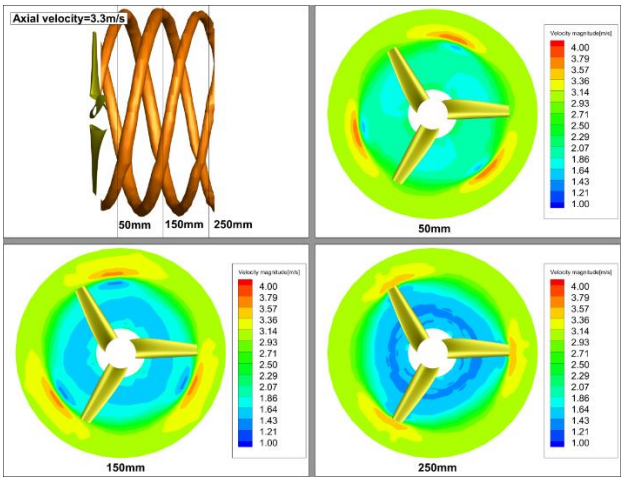

Figure 17. Velocity distribution for the reference turbine at varied sections, 50mm, 150mm and 250mm downstream of model turbine at TSR4 with the iso-surface of axial velocity = 3.3m/s

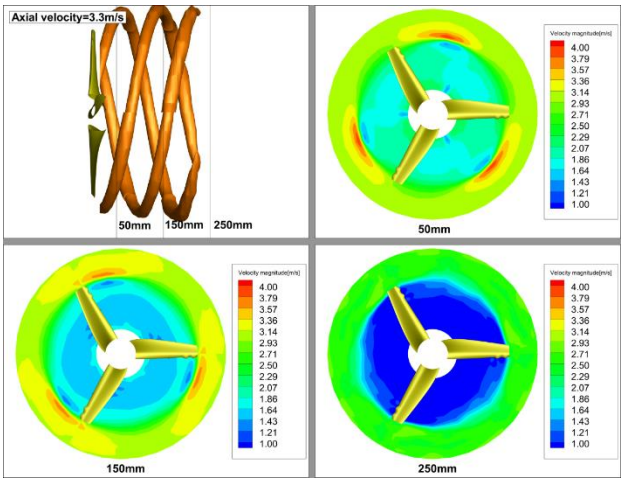

Figure 18. Velocity distribution for the Sin2 turbine at varied sections, 50mm, 150mm and 250mm downstream of model turbine at TSR4 with the iso-surface of axial velocity = 3.3m/s

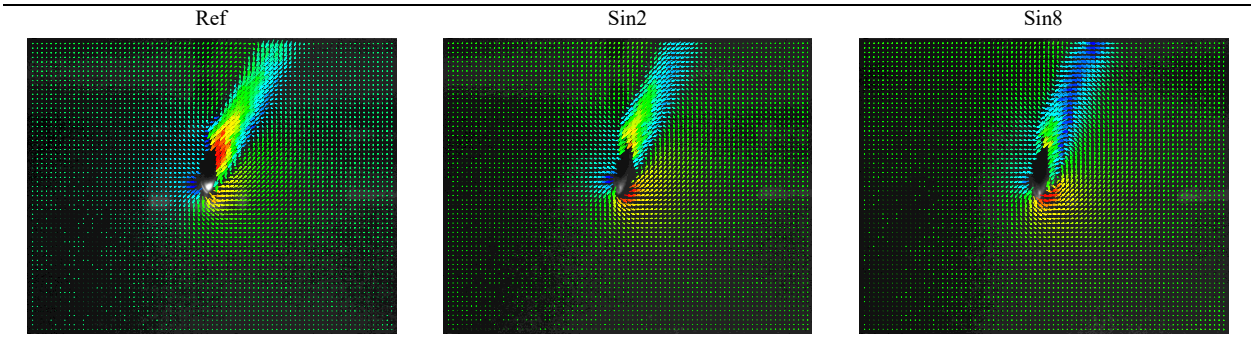

Fig. 16 PIV measurement of the cross-section at 0.9r of the three models at TSR=2 and V=4m/s

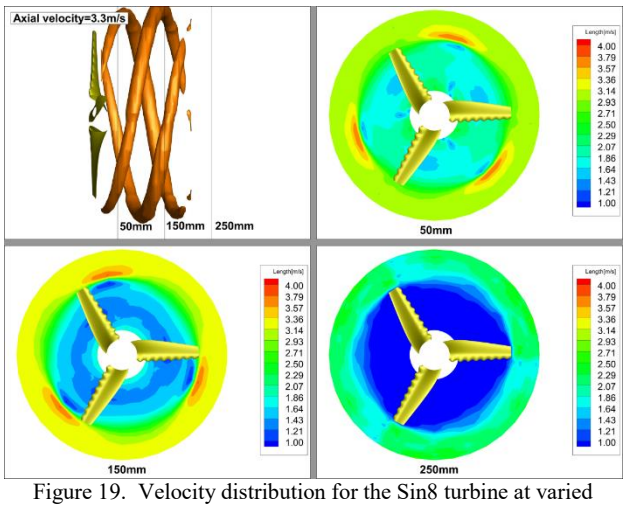

Figure 19. Velocity distribution for the Sin8 turbine at varied sections, 50mm, 150mm and 250mm downstream of model turbine at TSR4 with the iso-surface of axial velocity = 3.3m/s

PIV measurements in Figure 17 to Figure 19 also revealed that the tip vortex was weakened and its axial trajectory was shortened by the tubercles in the "Optimum working condition" (TSR=4 and V=3m/s). This was further confirmation of the reduced 3D effects of the actual turbine blades by the tubercles, reflecting the findings in Section 3. This finding is also positively related to the number of tubercles.

5 CONCLUSIONS

By going through a comprehensive set of experimental investigations for full turbine model with and without the leading edge tubercles, the comparative hydrodynamic efficiencies were investigated including the cavitation and underwater noise performances in current only. These investigations were supported with comprehensive flow analyses using the state-of-the-art experimental tools for further exploration and understanding of the effects of tubercles on tidal turbines as well as presenting a bench mark data for future research and developments.

Investigations conducted in this paper proved the beneficial effects on various hydrodynamic performances of these turbines with leading edge tubercles, mainly with improved performance in low TSRs without influencing the maximum power coefficient, limited cavitation development and hence lowered noise level. Based on this model scale demonstration, this bionic concept is ready for the next really sea applications.

ACKNOWLEDGEMENT

This research is funded by the School of Marine Science and Technology, Newcastle University and China Scholarship Council. Hence the financial support obtained from both establishments is gratefully acknowledged. The Authors would like to thank all the team members in the Emerson Cavitation Tunnel for the help in testing and sharing their knowledge. And the last but not the least, special acknowledgement to the team in Strathclyde University. Thanks for the support for the last stage of this study.

REFERENCE

Hansen, K., Kelso, R., & Doolan, C. (2012). Reduction of Flow Induced Airfoil Tonal Noise Using Leading Edge Sinusoidal Modifications. *Acoustics Australia*, *40*(3), 172-177.

Hansen, K. L., Kelso, R. M., & Dally, B. B. (2009). *The effect of leading edge tubercle geometry on the performance of different airfoils*. Paper presented at the ExHFT-7, Krakow, Poland.

Hansen, K. L., Kelso, R. M., & Dally, B. B. (2011). Performance Variations of Leading-Edge Tubercles for Distinct Airfoil Profiles. *Aiaa Journal*, *49*(1), 185-194. doi:10.2514/1.J050631

Hansen, K. L., Rostamzadeh, N., Kelso, R. M., & Dally, B. B. (2016). Evolution of the streamwise vortices generated between leading edge tubercles. *Journal of Fluid Mechanics*, *788*, 730-766. doi:10.1017/jfm.2015.611

Pham, X., Clelland, D., Grant, A., Varyani, K. S., & Barltrop, N. (2006). Wave-current interactions in marine current turbines. *Proceedings of the Institution of Mechanical Engineers, Part M: Journal of Engineering for the Maritime Environment*, *220*(4), 195-203. doi:10.1243/14750902jeme45

Shi, W., Atlar, M., Norman, R., Aktas, B., & Turkmen, S. (2016). Numerical optimization and experimental validation for a tidal turbine blade with leading-edge tubercles. *Renewable Energy*, *96*, 42-55.

Shi, W., Rosli, R., Atlar, M., Norman, R., Wang, D., & Yang, W. (2016). Hydrodynamic performance evaluation of a tidal turbine with leading-edge tubercles. *Ocean Engineering*, *117*, 246-253. doi:10.1016/j.oceaneng.2016.03.044

Stanway, M. J. (2008). *Hydrodynamic effects of leading-edge tubercles on control surfaces and in flapping foil propulsion.* (Msc), Massachusetts Institute of Technology.

Swanson, T., & Isaac, K. M. (2011). Biologically Inspired Wing Leading Edge for Enhanced Wind Turbine and Aircraft Performance: AIAA.

van Nierop, E. A., Alben, S., & Brenner, M. P. (2008). How bumps on whale flippers delay stall: an aerodynamic model. *Phys Rev Lett*, *100*(5), 054502. doi:10.1103/PhysRevLett.100.054502

Wang, D., Atlar, M., & Sampson, R. (2007). An experimental investigation on cavitation, noise, and slipstream characteristics of ocean stream turbines. *Proceedings of the Institution of Mechanical Engineers Part a-Journal of Power and Energy*, *221*(A2), 219-231. doi:10.1243/09576509jpe310

DISCUSSION

Question from Zhihui Liu

Does the difference in flow separation points along the spanwise direction help to improve the C_L?

Author's closure

From the current study, we orbserved both more attached flow and constrained 3D flow. Therefore, the improve of the lift coefficient in the post stall conditions is accredit to both flow mechanisms.

Question from Mike Kries

Do you see the reattachment at the peak of the tubercles or the valleys improves stall performance?

Author's closure

Yes, we can confirm the reattachment of the flow can increase the performance. We have published the finding in the following paper, where we analyzed the pressure distribution along the 3D hydrofoil, and found the reattachment will create high suction force on the suction side without changing the pressure force.

Shi, W., et al. (2016). Numerical simulation of a tidal turbine based hydrofoil with leading-edge tubercles. 35th International Conference on Ocean, Offshore and Arctic Engineering, OMAE2016. Busan, Korea, Proceedings of the ASME 2016.

Question from Martin Greeve

Did the medium chord length of the modified foil match the chord length of the reference foil, or increase?

Author's closure

The averaged chord length will be increased by 5% for the design Sin8 and by 0.9% for the design Sin2. But it should not be the reason for the performance improvement. Because the increase of the chord length won't improve the stall performance.